

Published in final edited form as:

Oncogene. 2013 September 5; 32(36): 4319–4324. doi:10.1038/onc.2012.447.

Platelets govern pre-metastatic tumor communication to bone

Bethany A. Kerr, Ph.D.¹, N. Patrick McCabe, Ph.D.¹, Weiyi Feng, M.D., Ph.D.^{1,2}, and Tatiana V. Byzova, Ph.D.^{1,3}

¹Department of Molecular Cardiology, Joseph J. Jacobs Center for Thrombosis and Vascular Biology, Lerner Research Institute, The Cleveland Clinic

²The First Affiliated Hospital, School of Medicine, Xi'an Jiaotong University, Xi'an, Shaanxi China

³Taussig Cancer Center, The Cleveland Clinic, Cleveland, OH

Abstract

While the survival rate for early detected cancers is high, once a cancer metastasizes to bone, it is incurable. Interestingly, patients without visible metastases display abnormal bone formation and resorption suggesting a link between primary cancers and the bone microenvironment prior to metastasis and this link likely facilitates preparation of the pre-metastatic niche. We hypothesized that communication from the primary tumor would result in bone remodeling alterations and that platelets could facilitate this communication. Using three tumor models, we demonstrate that primary tumor growth stimulates bone formation measured by microcomputed tomography (microCT). Further, platelet depletion prevented tumor-induced bone formation highlighting the importance of platelets in the communication between tumors and the bone microenvironment. Finally, we determine that platelets sequester a variety of tumor-derived proteins, TGF- β 1 and MMP-1 in particular, which regulate bone formation. Thus, our data reveals that platelets function as mediators of tumor-bone communication prior to metastasis.

Keywords

platelet; bone metastasis; bone remodeling; tumor

INTRODUCTION

Approximately 80% of advanced prostate cancers and 25–49% of advanced melanomas metastasize to the skeleton causing pain in the hips, spine, ribs, or other bones (1, 2). Once a cancer produces bone metastases, it becomes incurable (3). Both prostate cancer and melanoma have survival rates of approximately 100% if localized when diagnosed. However, the five year survival rate drops to 30% for prostate cancer and 16% for melanomas once distant metastases have developed (4). Interestingly, a majority of patients with prostate cancer are found to have a significant number of tumors within the bone at autopsy, although they are largely asymptomatic. In patients, primary prostate cancer induces the abnormal formation and turnover of bone prior to metastasis (5). The growth of primary tumors are aided by the presence of a variety of factors sequestered in and released

Reprint Requests: Tatiana Byzova, Ph.D., The Cleveland Clinic, NB-50, 9500 Euclid Avenue, Cleveland, OH, 44195. Telephone: 216-445-4312; Fax: 216-445-8204; byzovat@ccf.org.

Present Affiliations: N.P. McCabe: Department of Neurology, Case Western Reserve University, Cleveland, OH 44106

CONTRIBUTIONS B.A.K.: designed and performed research, analyzed data, wrote the paper; N.P.M. and W.F.: performed research, analyzed data; T.V.B.: designed research, analyzed data, wrote the paper.

Supplementary Information accompanies the paper on the Oncogene website (<http://nature.com/onc>).

from the bone matrix during remodeling and those produced by activated osteoclasts and osteoblasts; such as parathyroid hormone-related protein, RANKL, TGF- β 1, basic fibroblast growth factor, insulin-like growth factor, Ca²⁺, and osteonectin/SPARC (6). Thus, the cancer cells and bone microenvironment interact in a positive-feedback cycle to enhance tumor aggressiveness.

Vascularization of the primary tumor and metastasis of cancer cells through the blood stream allow for interaction between the cancer cells and platelets. Further, metastatic tumor cells may travel through the bloodstream as small thrombi with platelets (7) for protection against shear stress. In addition, platelets are activated within tumors, where they may release or acquire proteins. The releasate of platelets contains anti- and pro-angiogenic factors, such as VEGF, TGF- β 1, and thrombospondin-1, which can control tumor growth. Increased levels of VEGF in the serum and platelets directly correlates with increased tumor metastasis (8). We have recently shown that platelets mediate tumor communication with the bone marrow resulting in bone-marrow derived cell mobilization (9). Proteins released from activated platelets can also function directly on bone stimulating proliferation of osteoblasts, inducing regeneration of bone (10, 11), and promoting the differentiation of osteoclast-like cells (12). Further, platelet-rich plasma, which contains activated and resting platelets, stimulates mesenchymal stem cell osteogenesis (13). Thus, platelets may play an important role in the growth of primary tumors and facilitate the tumor spread by preparing the future metastatic site.

Despite the progress made over the last decade in the treatment of cancer, the mechanisms governing its metastatic development in bone remain enigmatic. Recent clinical evidence indicates that the primary tumors communicate with bone prior to metastasis. However, the participating players in the crosstalk between tumor and the bone microenvironment that mediate tumor homing and contribute to tumor growth within the skeleton remain to be determined. In this study, we elucidate the effects of primary tumor growth on bone metabolism using murine prostate cancer (RM1) or murine melanoma (B16-F10) cells implanted in immunocompetent mice or human prostate cancer (LNCaP-C4-2) cells implanted in immunocompromised mice. These three different tumor models were used to assess changes in bone structure induced by distal tumor. Using platelet depletion, we demonstrate that platelets are required for tumor-induced bone formation and using our xenograft model we identify tumor-derived proteins sequestered in platelets that may be responsible for tumor-induced bone formation.

RESULTS AND DISCUSSION

Primary tumor growth stimulates bone formation

We have previously demonstrated that direct injection of tumors into the bone environment results in alterations in bone turnover (14–16). Cancer cells are more likely to colonize bone during the remodeling period (17); thus, it would benefit the tumor to stimulate bone turnover prior to metastasis. However, established cancer metastases can be either osteoblastic or osteolytic. In our previous studies, intratibial injection of murine prostate cancer RM1 cells resulted in osteolysis (14, 16), while human prostate cancer LNCaP-C4-2 injection resulted in bone formation (15). In the present study, we determined the effects of distal, primary tumor growth on bone turnover. Using three models: murine RM1 prostate cancer and murine B16-F10 melanoma in immunocompetent mice and human LNCaP-C4-2 prostate cancer in immunodeficient mice, we measured bone structural indices in mice one day before and 9, 12 or 19 days for B16-F10, RM1 and LNCaP-C4-2, respectively, after tumor implantation (Figure 1A and Supplemental Table 1). The bone structural indices were not significantly between the groups at the initial time point. As measured by microCT, bone volume to total volume ratio (BV/TV) at the final time point was increased in mice bearing

tumors for all models, 1.28 fold for B16-F10, 1.63 fold for RM1, and 1.79 fold for LNCaP-C4-2 injected mice compared with control (Figure 1B). Bone surface area (BSA) was increased in B16-F10, RM1 and LNCaP-C4-2 implanted mice 1.62, 1.21, and 1.75 fold, respectively, compared with control mice (Figure 1C). Trabecular thickness (Tb.Th) was increased in RM1 and LNCaP-C4-2 injected mice compared with controls, 1.37 and 1.23 fold, respectively (Figure 1D). Interestingly, melanoma injected mice displayed increases in trabecular number (Tb.N) (1.29 fold), while the prostate cancer injected mice demonstrated no significant change in Tb.N compared with control (Figure 1E). To confirm that the increased bone in mice bearing tumors was due to osteoblast activation, plasma concentrations of osteocalcin and bone alkaline phosphatase were measured (Figure 2). Osteocalcin was increased in B16-F10, RM1 and LNCaP-C4-2 implanted mice 1.44, 1.25, and 1.48 fold respectively compared with control mice (Figure 2A). Correspondingly, bone alkaline phosphatase was increased in B16-F10, RM1 and LNCaP-C4-2 implanted mice 1.53, 1.49, and 1.20 fold respectively compared with control mice (Figure 2B). During the same period, plasma calcium concentrations were altered slightly with levels being increased in immunocompetent mice and decreased in the immunocompromised mice (Supplemental Figure 1). Together, our data demonstrates that distal tumor growth stimulates bone formation in three different *in vivo* tumor models. This data has been confirmed clinically by studies demonstrating that primary tumors stimulate abnormal bone formation in patients (5). Although it is known that prostate cancer cells preferentially metastasize to trabecular bone and cause osteoblastic lesions (18, 19), this is the first report showing that other tumors, i.e. melanomas, are capable of changing the bone structure.

Platelet depletion inhibits tumor-induced bone formation

We next addressed the mechanism of distal tumor communication with the bone tissue by testing our hypothesis that this interaction is mediated by circulating platelets. Indeed, platelet contents are known to stimulate bone formation during fracture repair (10, 11), and we have recently shown the role of platelets in communications between ischemic tissues and bone marrow (9). Using our B16-F10 tumor model, we depleted platelet levels using a GPIIb/IIIa antibody to diminish platelet levels by 90% compared with control IgG, as shown previously by us (20) and others (21). We chose to focus on the B16-F10 tumor model because its changes in Tb.N and Tb.Sp with no significant change in Tb.Th indicate *de novo* bone formation (Figure 1), in which bone forms in a process similar to fracture repair. We found that BV/TV was increased 1.51 fold in mice bearing tumors compared with control (Figure 3A and B). Platelet depletion prevented tumor-induced bone formation, since levels of BV/TV, Tb.N, and BSA in platelet depleted animals were similar to control animals without tumor (Figure 3 and Supplemental Table 2). However, platelet infusion was unable to significantly increase bone formation over that already induced by the tumor (Supplemental Table 2). In addition, platelet depletion in control mice not bearing tumors had no effect on bone structure (data not shown). Our data indicate that platelets are necessary for tumor-induced bone formation. Diminishing platelet levels correlated with a decrease in the development of metastases in mice (22). In addition, inhibiting the ability of platelets to bind tumor cells results in a decreased number of cells colonizing metastatic tissues (23). Further, incubation of bone-marrow derived cells with platelet releasates results in increased cell migration and proliferation (24), which may cause osteogenesis during bone regeneration. During fracture healing, increasing levels of platelets in platelet-rich plasma gel results in improved bone formation, non-union closure, and mineralization of the callus (10). Further, platelet-rich plasma stimulates both mesenchymal stem cell and osteoblast proliferation and differentiation (11, 25). Correspondingly, when we treated murine osteoblast MC3T3-E1 cells with platelet releasates from mice bearing B16-F10 tumors, osteoblast mineralization was significantly increased (Figure 3F). Thus, proteins

released upon platelet activation may stimulate osteoblast differentiation resulting in increased bone formation.

Platelets sequester proteins related to bone metabolism

Our findings demonstrate that platelets are required for bone formation in response to tumor growth. Importantly, platelets are able to accumulate proteins within their α granules regardless of a concentration gradient and segregate these proteins resulting in differential release to stimulate specific pathways in recipient cells (26, 27). We used a tumor xenograft model to determine what tumor-produced factors sequestered by platelets were capable of modulating bone formation. Using our LNCaP-C4-2 model, platelets were isolated from whole blood, lysed, and assayed using an ELISA-based, human-specific protein array to determine the levels of tumor-derived proteins within platelets. Several factors associated with bone metabolism were found to be tumor-derived and present within platelet lysates. No human-derived proteins were measured in control animals, demonstrating the assay specificity (Figure 4A). We have also measured VEGF, G-CSF, and MMP-9 in the range of 130 to 1,050 pg/mL in platelet lysates from tumor-bearing mice (9). Remarkably, TGF- β 1 was present at the highest concentration in the platelet compartment (Figure 4A). TGF- β 1 promotes tumor progression and skeletal metastasis of several cancers (28, 29). Our analysis showed that TGF- β 1 was produced by the tumor and was present at 126,425 pg/mL in the platelet lysates of tumor-bearing mice (Figure 4A). In agreement with previous studies, it appears that platelets serve as a key reservoir of TGF- β 1 in the circulation (30, 31). TGF- β 1 stimulates osteoblast maturation, proliferation, and subsequent bone formation, suggesting an important role in tumor-induced bone formation. VEGF also stimulates osteoblast maturation and initial matrix calcification (32). TGF- β 1 treatment promotes bone formation *in vivo* (33). TGF- β 1 stimulation induces VEGF production in osteoblast-like cells, which may further stimulate bone formation (32, 34, 35). MMP-1, MMP-3, MMP-13, and tissue inhibitor of metalloproteinase (TIMP)-2 concentrations in platelet lysates ranged from approximately 13,750 to 210 pg/mL (Figure 4A). MMPs produced by the tumor may degrade the bone matrix leading to release of IGF, TGF- β 1, and BMPs resulting in osteoblast mobilization and mineralization. In addition the exposed bone matrix recruits osteoblasts to repair the bone resulting in increased bone formation (36). MMP-1, MMP-13, TIMP-1, and TIMP-2 are expressed by osteoblasts at the base of the growth plate (37). TIMPs are involved in bone formation and may neutralize excessive bone degradation by the MMPs. RANK and RANKL are believed to target bone tissues and control tumor metastasis (38, 39) and were present at approximately, 5,200 and 625 pg/mL, respectively (Figure 4). RANKL was tumor-derived and may stimulate osteoclast differentiation resulting in further release of trapped growth factors from the bone matrix; thus potentially stimulating osteoblasts and prostate cancer cells. Tumors also produce soluble RANK, which would compete with osteoclasts for RANKL and may diminish the effects of RANKL production. To confirm that platelet-derived TGF- β 1 and MMP-1 are increased in mice bearing tumors, we measured the concentrations of the two proteins in platelet releasates. TGF- β 1 levels were significantly higher in mice bearing the prostate cancer, while it was slightly decreased in mice bearing melanoma (Supplemental Figure 2A and B). MMP-1 levels, conversely, were highly elevated in mice with B16-F10 tumors and not significantly changed in RM1 implanted mice (Supplemental Figure 2C). In addition to these increases in bone remodeling factors in platelets, in response to some tumor types, but not others, the MMPs and TGF- β 1 were also increased in the plasma of tumor bearing mice ((40) and data not shown) and thus, there remains a possibility that plasma-derived proteins are also contributing to altered bone remodeling. These data indicate that the proteins sequestered within platelets and circulating in plasma in response to tumors may be specific to individual tumor types. Further, the xenograft model demonstrates that tumor-derived proteins can be internalized by and sequestered within platelets. Thus, it appears that communication

between tumor and bone are mediated by platelets as carriers of factors stored in their granules.

To determine whether these tumor-derived human proteins could affect osteoblast differentiation and function, we treated murine MC3T3-E1 osteoblast cells with ascorbic acid to induce differentiation in the presence of platelet releasates from mice bearing LNCaP-C4-2 tumors. These cells were further treated with human-specific neutralizing antibodies for MMP-1 and TGF- β 1, in addition to the broad MMP inhibitor marimastat, to inhibit the tumor-derived proteins found at the highest concentration in platelets (Figure 4A). The treatment of osteoblasts with platelet releasates from tumor bearing mice significantly increased osteoblast differentiation after 14 days of culture as shown by alizarin red staining (Figure 4B). Broad MMP inhibition using marimastat significantly inhibited osteoblast function in cultures treated with tumor-derived proteins (Figure 4B). Neutralization of TGF- β 1 decreased alizarin red staining in the cultures treated with platelet releasates, with no effect in control cultures (Figure 4B). Neutralization of MMP-1 slightly decreased osteoblast function in cultures treated with platelet releasates (Figure 4B). The inhibitors had no effect on control cultures, indicating that only the human proteins from the tumor present in platelet releasates were being affected. Interestingly, specifically blocking only the tumor-derived TGF- β 1 and MMPs, with the growth factors in serum and those produced by the MC3T3-E1 cells still available, resulted in significant decreases in osteoblast function. These data demonstrate that inhibition of tumor-derived proteins can have profound effects on osteoblast differentiation and function, underscoring the potential of these tumor-derived proteins to be targeted in treatments to prevent metastasis.

In conclusion, we demonstrate that distal tumors are able to change bone structure by means of circulating platelets. Primary tumor growth stimulated increased BV/TV in three distinct tumor models. Platelet depletion inhibited bone formation in response to tumor growth. BV/TV and Tb.N are increased in mice bearing tumors; however depletion of platelets results in BV/TV and Tb.N levels similar to mice without tumors. Using a xenograft model and species-specific protein arrays, we demonstrate that platelets uptake high concentrations of tumor-secreted proteins associated with the control of bone metabolism. Thus, platelets regulate the bone formation induced by tumors through uptake of tumor-derived proteins and likely through the secretion of their α granule contents possibly resulting in osteoblast differentiation and maturation. This pre-metastatic communication identifies a possible therapeutic target for controlling or detecting early metastasis, which, in turn, will improve the survival rates of cancer patients.

Supplementary Material

Refer to Web version on PubMed Central for supplementary material.

Acknowledgments

We thank Miroslava Tischenko, Steven Maximuk, and Richard Rozic for technical assistance. Dr. Amit Vasanji developed the software and techniques for microCT analysis. Cleveland Clinic Biomedical Imaging and Analysis Core Center was funded in part by NIAMS Core Center Grant 1P30 AR050953. B.A.K was supported by a Ruth L. Kirschstein NRSA award (F32 CA142133) from the NIH/NCI. N.P.M. was supported by a Ruth L. Kirschstein NRSA award (F32 CA117262). This study was supported by research funding from the NIH/NCI (grant CA126847) to T.V.B.

CONFLICT OF INTEREST Dr. Byzova's work has been funded by the NIH. Dr. Kerr and Dr. McCabe have been awarded fellowships from the NIH.

Abbreviations

BSA	bone surface area
BV/TV	ratio of bone volume to total volume
microCT	microcomputed tomography
Tb.Th	trabecular thickness
Tb.N	trabecular number
Tb.Sp	trabecular spacing
TIMP	tissue inhibitor of metalloproteinase

REFERENCES

1. American Cancer Society. Prostate Cancer. American Cancer Society; Atlanta, GA: 2008.
2. American Cancer Society. Melanoma Skin Cancer. American Cancer Society; Atlanta, GA: 2008.
3. Coleman RE, Guise TA, Lipton A, Roodman GD, Berenson JR, Body J-J, et al. Advancing Treatment for Metastatic Bone Cancer: Consensus Recommendations from the Second Cambridge Conference. *Clin Cancer Res.* 2008; 14(20):6387–95. [PubMed: 18927277]
4. Siegel R, Ward E, Brawley O, Jemal A. Cancer statistics, 2011: the impact of eliminating socioeconomic and racial disparities on premature cancer deaths. *CA Cancer J Clin.* Jul-Aug;2011 61(4):212–36. [PubMed: 21685461]
5. Kingsley LA, Fournier PGJ, Chirgwin JM, Guise TA. Molecular Biology of Bone Metastasis. *Mol Cancer Ther.* 2007; 6(10):2609–17. [PubMed: 17938257]
6. Mundy GR. Metastasis to Bone: Causes Consequences and Therapeutic Opportunities. *Nat Rev Cancer.* 2002; 2:584–93. [PubMed: 12154351]
7. Karpatkin S, Pearlstein E, Ambrogio C, Collier BS. Role of Adhesive Proteins in Platelet Tumor Interaction In Vitro and Metastasis Formation In Vivo. *J Clin Invest.* 1988; 81:1012–9. [PubMed: 3280598]
8. Borsig L. The Role of Platelet Activation in Tumor Metastasis. *Exp Rev Anticancer Thers.* 2008; 8(8):1247–55.
9. Feng W, Madajka M, Kerr BA, Mahabeleshwar GH, Whiteheart SW, Byzova TV. A novel role for platelet secretion in angiogenesis: mediating bone marrow-derived cell mobilization and homing. *Blood.* Apr 7; 2011 117(14):3893–902. [PubMed: 21224474]
10. Kawasumi M, Kitoh H, Siwicka KA, Ishiguro N. The Effect of the Platelet Concentration in Platelet-Rich Plasma Gel on the Regeneration of Bone. *J Bone Joint Surg Br.* 2007; 90-B:966–72.
11. Uggeri J, Belletti S, Guizzardi S, Poli T, Cantarelli S, Scandroglio R, et al. Dose-Dependent Effects of Platelet Gel Release on Activities of Human Osteoblasts. *J Periodontol.* 2007; 78(10):1985–91. [PubMed: 18062120]
12. Gruber R, Karreth F, Fischer MB, Watzek G. Platelet-Released Supernatants Stimulate Formation of Osteoclast-like Cells through a Prostaglandin/RANKL-Dependent Mechanism. *Bone.* 2002; 30(5):726–32. [PubMed: 11996911]
13. Nair MB, Varma HK, John A. Platelet-Rich Plasma and Fibrin Glue-Coated Bioactive Ceramics Enhance Growth and Differentiation of Goat Bone Marrow-Derived Stem Cells. *Tissue Eng Part A.* 2009; 15(7):1619–31. [PubMed: 19072085]
14. McCabe NP, Madajka M, Vasanji A, Byzova TV. Intraosseous Injection of RM1 Murine Prostate Cancer Cells Promotes Rapid Osteolysis and Periosteal Bone Deposition. *Clin Exp Metastasis.* 2008; 25(5):581–90. [PubMed: 18506587]
15. McCabe NP, De S, Vasanji A, Brainard J, Byzova TV. Prostate Cancer Specific Integrin $\alpha_v\beta_3$ Modulates Bone Metastatic Growth and Tissue Remodeling. *Oncogene.* 2007; 26:6238–43. [PubMed: 17369840]

16. McCabe NP, Kerr BA, Madajka M, Vasanji A, Byzova TV. Augmented Osteolysis in SPARC-Deficient Mice with Bone-Residing Prostate Cancer. *Neoplasia*. Jan; 2011 13(1):31–9. [PubMed: 21245938]
17. Gomes RR Jr, Buttke P, Paul EM, Sikes RA. Osteosclerotic prostate cancer metastasis to murine bone are enhanced with increased bone formation. *Clin Exp Metastasis*. 2009; 26(7):641–51. [PubMed: 19421879]
18. Edlund M, Sung S-Y, Chung LW. Modulation of Prostate Cancer Growth in Bone Microenvironments. *J Cellular Biochem*. 2004; 91:686–705. [PubMed: 14991761]
19. Roudier MP, Morrissey C, True LD, Higano CS, Vessella RL, Ott SM. Histopathological Assessment of Prostate Cancer Bone Osteoblastic Metastases. *J Urol*. 2008; 180:1154–60. [PubMed: 18639279]
20. Feng W, McCabe NP, Mahabeleshwar GH, Somanath PR, Phillips DR, Byzova TV. The Angiogenic Response Is Dictated by β_3 Integrin on Bone Marrow-Derived Cells. *J Cell Biol*. 2008; 183(6):1145–57. [PubMed: 19075116]
21. Rhee JS, Black M, Schubert U, Fischer S, Morgenstern E, Hammes HP, et al. The functional role of blood platelet components in angiogenesis. *Thromb Haemost*. Aug; 2004 92(2):394–402. [PubMed: 15269837]
22. Gasic GJ, Gasic TB, Stewart CC. Antimetastatic Effects Associated with Platelet Reduction. *Proc Natl Acad Sci U S A*. 1968; 61(1):46–52. [PubMed: 5246932]
23. Borsig L, Wong R, Feramisco J, Nadeau DR, Varki NM, Varki A. Heparin and Cancer Revisited: Mechanistic Connections Involving Platelets, P-selectin, Carcinoma Mucins, and Tumor Metastasis. *Proc Natl Acad Sci U S A*. 2001; 98(6):3352–7. [PubMed: 11248082]
24. Oprea WE, Karp JM, Hosseini MM, Davies JE. Effect of platelet releasate on bone cell migration and recruitment in vitro. *J Craniofac Surg*. May; 2003 14(3):292–300. [PubMed: 12826799]
25. Mishra A, Tummala P, King A, Lee B, Kraus M, Tse V, et al. Buffered platelet-rich plasma enhances mesenchymal stem cell proliferation and chondrogenic differentiation. *Tissue Eng Part C Methods*. Sep; 2009 15(3):431–5. [PubMed: 19216642]
26. Italiano JE Jr, Richardson JL, Patel-Hett S, Battinelli E, Zaslavsky A, Short S, et al. Angiogenesis Is Regulated by a Novel Mechanism: Pro- and Antiangiogenic Proteins Are Organized into Separate Platelet α Granules and Differentially Released. *Blood*. 2008; 111(3):1227–33. [PubMed: 17962514]
27. Klement GL, Yip T-T, Cassiola F, Kikuchi L, Cervi D, Podust VN, et al. Platelets Actively Sequester Angiogenesis Regulators. *Blood*. 2009; 113(12):2835–42. [PubMed: 19036702]
28. Baselga J, Rothenberg ML, Taberner J, Seoane J, Daly T, Cleverly A, et al. TGF- β Signalling-Related Markers in Cancer Patients with Bone Metastasis. *Biomarkers*. 2008; 13(2):217–36. [PubMed: 18270872]
29. Shariat SF, Shalev M, Menesses-Diaz A, Kim IY, Kattan MW, Wheeler TM, et al. Preoperative Plasma Levels of Transforming Growth Factor Beta₁ (TGF- β_1) Strongly Predict Progression in Patients Undergoing Radical Prostatectomy. *J Clin Oncol*. 2001; 19(11):2856–64. [PubMed: 11387358]
30. Stellos K, Gawaz M. Platelet Interaction with Progenitor Cells: Potential Implications for Regenerative Medicine. *Thromb Haemost*. 2007; 98:922–9. [PubMed: 18000594]
31. Schultz-Cherry S, Murphy-Ullrich JE. Thrombospondin Causes Activation of Latent Transforming Growth Factor- β Secreted by Endothelial Cells by a Novel Mechanism. *J Cell Biol*. 1993; 122(4):923–32. [PubMed: 8349738]
32. Street J, Bao M, deGuzman L, Bunting S, Peale FV Jr, Ferrara N, et al. Vascular endothelial growth factor stimulates bone repair by promoting angiogenesis and bone turnover. *Proc Natl Acad Sci U S A*. Jul 23; 2002 99(15):9656–61. [PubMed: 12118119]
33. Joyce ME, Roberts AB, Sporn MB, Bolander ME. Transforming growth factor-beta and the initiation of chondrogenesis and osteogenesis in the rat femur. *J Cell Biol*. Jun; 1990 110(6):2195–207. [PubMed: 2351696]
34. Saadeh PB, Mehrara BJ, Steinbrech DS, Dudziak ME, Greenwald JA, Luchs JS, et al. Transforming growth factor-beta1 modulates the expression of vascular endothelial growth factor by osteoblasts. *Am J Physiol*. Oct; 1999 277(4 Pt 1):C628–37. [PubMed: 10516092]

35. Zelzer E, McLean W, Ng YS, Fukai N, Reginato AM, Lovejoy S, et al. Skeletal defects in VEGF(120/120) mice reveal multiple roles for VEGF in skeletogenesis. *Development*. Apr; 2002 129(8):1893–904. [PubMed: 11934855]
36. Sims NA, Gooi JH. Bone remodeling: Multiple cellular interactions required for coupling of bone formation and resorption. *Semin Cell Dev Biol*. Oct; 2008 19(5):444–51. [PubMed: 18718546]
37. Haeusler G, Walter I, Helmreich M, Egerbacher M. Localization of matrix metalloproteinases, (MMPs) their tissue inhibitors, and vascular endothelial growth factor (VEGF) in growth plates of children and adolescents indicates a role for MMPs in human postnatal growth and skeletal maturation. *Calcif Tissue Int*. May; 2005 76(5):326–35. [PubMed: 15868281]
38. Blouin S, Baslé MF, Chappard D. Interactions Between Microenvironment and Cancer Cells in Two Animal Models of Bone Metastasis. *Br J Cancer*. 2008; 98:809–15. [PubMed: 18253114]
39. Jones DH, Nakashima T, Sanchez OH, Kozieradzki I, Komarova SV, Sarosi I, et al. Regulation of Cancer Cell Migration and Bone Metastasis by RANKL. *Nature*. 2006; 440:692–6. [PubMed: 16572175]
40. Kerr BA, Miocinovic R, Smith AK, Klein EA, Byzova TV. Comparison of Tumor and Microenvironment Secretomes in Plasma and in Platelets during Prostate Cancer Growth in a Xenograft Model. *Neoplasia*. 2010; 12(5):388–96. [PubMed: 20454510]
41. Kerr, BA.; Byzova, TV. MicroCT: An Essential Tool in Bone Metastasis Research. In: Saba, L., editor. *Computed Tomography - Clinical Applications*. InTech; 2012. p. 211-30.
42. Reinholz GG, Getz B, Pederson L, Sanders ES, Subramaniam M, Ingle JN, et al. Bisphosphonates Directly Regulate Cell Proliferation, Differentiation, and Gene Expression in Human Osteoblasts. *Cancer Res*. 2000; 60:6001–7. [PubMed: 11085520]

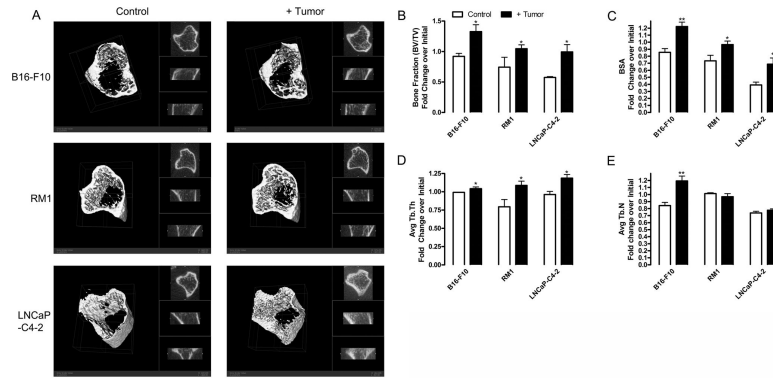


Figure 1. Distal tumor growth stimulates bone formation

Tumor cells were implanted subcutaneously into male mice: B16-F10 murine melanoma (2×10^6 cells in C57BL/6 mice, 9 wks of age), RM1 murine prostate cancer (4×10^5 cells in C57BL/6 mice, 9 wks of age), and LNCaPC4-2 human prostate cancer (4×10^5 cells encapsulated in matrigel in NOD/SCID mice, 8 wks of age) (black columns). Age-matched control mice were injected with PBS (for C57BL/6 mice) or matrigel (NOD/SCID mice) (white columns). Tibial bones were scanned using microCT prior to (*in vivo*) and upon experimental termination (*ex vivo*): 9 days (B16-F10), 12 days (RM1), or 19 days (LNCaP-C4-2) after tumor implantation. (A) Representative microCT scans of the analyzed metaphyseal area (first 20 slices cropped) from control and mice bearing B16-F10, RM1, or LNCaP-C4-2 at the final time point are shown. (B–E) Bone morphometric changes were measured using a GE Healthcare eXplore Locus MicroCT scanner with 360 X-ray projections collected at 1° increments and projected images reconstructed into 3D volumes at $20\mu\text{m}$ resolution as previously described (14, 16, 41) for (B) bone volume: total volume ratio (BV/TV), (C) bone surface area (BSA), (D) average trabecular thickness (Avg Tb.Th), and (E) average trabecular number (Avg Tb.N). Values are represented as fold change over initial measurements \pm SEM ($n=5$). * $p < 0.05$ and ** $p < 0.01$ vs. control by paired Student's *t* test (GraphPad Prism 4.03 software, La Jolla, CA).

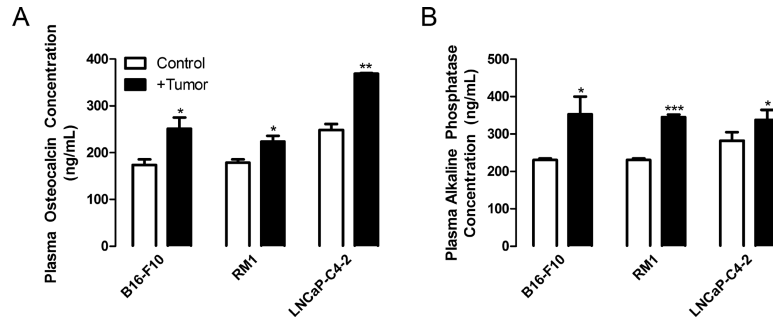


Figure 2. Distal tumor growth increases markers of bone formation

Plasma was isolated from control injected mice or mice bearing RM1, B16-F10 or LNCaP-C4-2 tumors upon experimental termination and subjected to (A) Life Sciences Advanced Technologies (St. Petersburg, FL) Blue Gene Osteocalcin ELISA or (B) Blue Gene Bone Alkaline Phosphatase ELISA assays to measure the concentration of proteins represented as mean \pm SEM ($n=2-3$). * $p<0.05$ and *** $p<0.005$ vs. control by unpaired Student's t test.

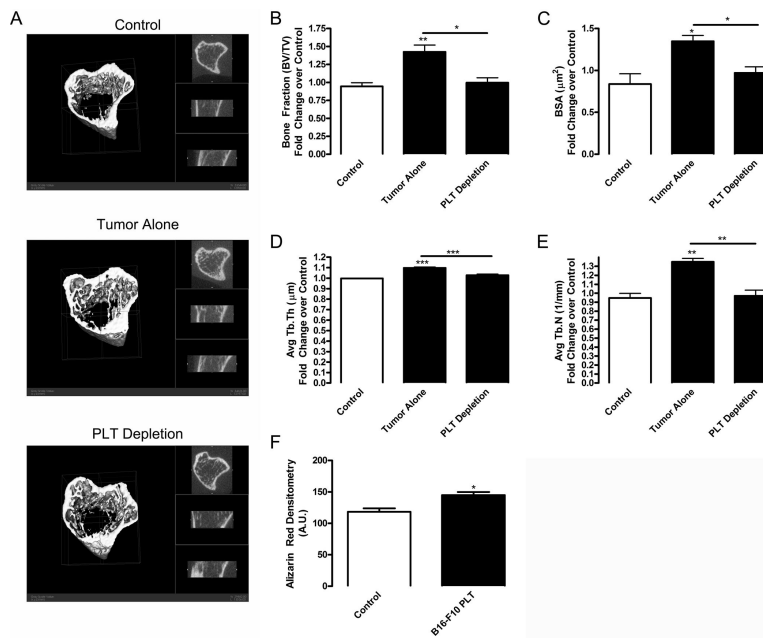


Figure 3. Platelet depletion inhibits tumor-induced bone formation

B16-F10 (2×10^6) tumor cells were implanted subcutaneously in 9 wk old C57BL/6 mice (black columns). Control mice were injected with PBS (white column). After tumor implantation, mice were treated with rat anti-mouse GPIIb/IIIa (PLT Depletion) or rat IgG (Tumor Alone and Control) ($2 \mu\text{g/g}$ body weight, each, Emfret Analytics, Eibelstadt, Germany) by tail vein injection. Injections were repeated every 3 days. Tibial bones were scanned using microCT prior to (*in vivo*) and 9 days after tumor implantation (*ex vivo*). (A) Representative microCT scans of bones from control, tumor alone, and platelet depleted mice at the final time point are shown (first 20 slices cropped). Bone morphometric changes were measured using a GE Healthcare eXplore Locus MicroCT scanner with 360 X-ray projections collected at 1° increments and projected images reconstructed into 3D volumes at $20 \mu\text{m}$ resolution for (B) bone volume: total volume ratio (BV/TV), (C) bone surface area (BSA), (D) average trabecular thickness (Avg Tb.Th), and (E) average trabecular number (Avg Tb.N). Values are represented as mean fold change over control \pm SEM ($n=4$). * $p < 0.05$ and ** $p < 0.01$ vs. control or tumor alone samples by paired Student's *t* test. (F) Osteoblast MC3T3-E1 cells on collagen I coated plates were differentiated for 14 days using $50 \mu\text{M}$ ascorbic acid (Wako, Richmond, VA) in the presence of control or 1% activated platelet releasate collected from mice bearing B16-F10 tumors (B16-F10 PLT). To induce mineralization, 10 mM β -glycerophosphate (Sigma, St. Louis, MO) was added after day 6. Alizarin red staining for mineralization was performed as previously described (42). Densitometry of staining was performed using NIH ImageJ and represented as mean arbitrary units (A.U.) \pm SEM ($n=2-3$). * $p < 0.05$ vs. control by unpaired Student's *t* test.

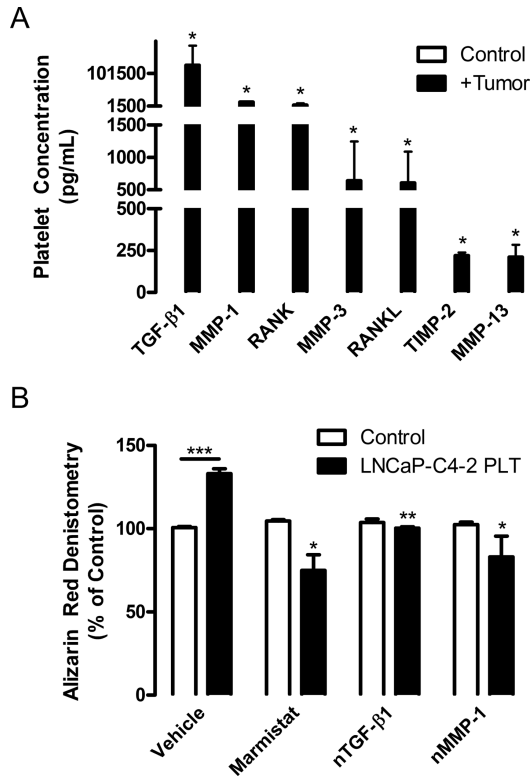


Figure 4. Platelets sequester tumor-derived proteins responsible for bone turnover

(A) NOD/SCID mice were injected subcutaneously with 4×10^5 human LNCaP-C4-2 cells. After 28 days of tumor growth, platelets were isolated from whole blood of control (white columns) and tumor bearing (black columns) mice by centrifugation and lysed in RIPA buffer (Sigma) containing 1 mM protease inhibitors. The resulting lysates were assayed with a custom-designed Quantibody human-specific protein array from RayBiotech (Norcross, VA) to detect tumor-derived proteins according to the manufacturer's protocol. Values were extracted using the Axon Gene Pix Pro 4.1 software and analyzed using the RayBiotech Custom Raybio Q-Analyzer software, which uses standardized dilutions of each protein to create standard curves used in determining the concentration in pg/mL of each protein in the samples; represented as mean values \pm SEM ($n=4$). No tumor-derived proteins were found in the platelets of control mice, demonstrating the specificity of the array. * $p < 0.05$ vs. control by unpaired Student's *t* test. (B) Osteoblast MC3T3-E1 cells on collagen I coated plates were differentiated using 50 μ M ascorbic acid in the presence of control or 1% activated platelet releasate collected from mice bearing LNCaP-C4-2 tumors (LNCaP-C4-2 PLT). Cultures were grown in the presence of 1 μ g/mL anti-human MMP-1 neutralizing antibody (nMMP-1; R&D Systems, Minneapolis, MN), 0.6 μ M marimastat (Sigma), 1 μ g/mL anti-human TGF- β 1 neutralizing antibody (nTGF- β 1; R&D Systems), or vehicle control for 14 days. To induce mineralization, 10 mM β -glycerophosphate was added after day 6. Alizarin red staining for mineralization was performed as previously described (42). Densitometry of staining was performed using NIH ImageJ and represented as mean % of control \pm SEM ($n=2-3$). * $p < 0.05$, ** $p < 0.01$, and *** $p < 0.005$ vs. control or vehicle by unpaired Student's *t* test.